Groundwater Monitoring&Remediation

Hydraulic Performance of the Horizontal Reactive Media Treatment Well: Pilot and Numerical Study

by Blossom N. Nzeribe, Wen Li, Michelle Crimi, Guangming Yao, Craig E. Divine, Jeff McDonough, and Jack Wang

Abstract

This study is focused on a passive treatment system known as the horizontal reactive treatment well (HRX Well®) installed parallel to groundwater flow, which operates on the principle of flow focusing that results from the hydraulic conductivity (K) ratio of the well and aquifer media. Passive flow and capture in the HRX Well are described by simplified equations adapted from Darcy's Law. A field pilot-scale study (PSS) and numerical simulations using a finite element method (FEM) were conducted to verify the HRX Well concept and test the validity of the HRX Well-simplified equations. The hydraulic performance results from both studies were observed to be within a close agreement to the simplified equations and their hydraulic capture width approximately five times greater than the well diameter (0.20 m). Key parameters affecting capture included the aquifer thickness, well diameter, and permeability ratio of the HRX Well treatment media and aquifer material. During pilot testing, the HRX Well captured 39% of flow while representing 0.5% of the test pit cross-sectional volume, indicating that the well captures a substantial amount of surrounding groundwater. While uncertainty in the aquifer and well properties (porosity, K, well losses), including the effects of boundary conditions, may have caused minor differences in the results, data from this study indicate that the simplified equations are valid for the conceptual design of a field study. A full-scale HRX Well was installed at Site SS003 at Vanderberg Air Force Base, California, in July/August 2018 based on outcomes from this study.

Introduction

Hantush and Papadopulos (1962) were the first to investigate the use of horizontal wells for contaminant removal in groundwater. The use of horizontal wells has gained considerable attention in recent years because horizontal wells offering certain advantages over vertical wells, such as ease of accessibility of a contaminated zone and lower operating and monitoring costs (Zhan 1999; Zhan and Zlotnik 2002; Chen et al. 2003). One of the reasons that horizontal wells are effective in groundwater remediation is that most environmental contaminants are within 100 feet of the surface, and plumes are planar in nature (Sawyer and Lieuallen-Dulam 1998; Zhan 1999; Payne et al. 2008). Consequently, it often takes an array of numerous vertical wells to achieve the same linear footage of well screen in contact with the contaminants as a few horizontal wells (Zhan and Zlotnik 2002; Kompani-Zare et al. 2005; Laton 2019), potentially reducing the cost associated with installation and operation. Specifically, for groundwater remediation, horizontal wells are used in groundwater extraction, air sparging, chemical injection, and bioremediation strategies (Furukawa et al. 2017). Despite their advantages, there have been concerns over the cost associated with drilling horizontal wells (Cleveland 1994; Allouche et al. 1998; Ariaratnam and Allouche 2000; Koenigsberg et al. 2018). However, newer drilling methods, such as horizontal directional drilling (HDD), have helped offset these costs. HDD is a robust, sustainable, and proven strategy that has become a successful tool in groundwater remediation (Lubrecht 2012). Lubrecht (2012) provides a comprehensive description of HDD as a green and sustainable technology for site remediation.

In addition to advanced drilling methods, improvements are being made to the traditional application of horizontal wells for groundwater remediation. Divine et al. (2013, patent US 8596351 B2) developed a novel concept of using conventional horizontal wells for in situ groundwater remediation. This technology is known as the Horizontal Reactive Treatment Well (HRX Well®) (Divine et al. 2013) and involves the installation of a large diameter horizontally drilled well filled with a granular reactive media within a contaminant plume. The well is installed in the direction of groundwater flow. Due to the "flow focusing" behavior resulting from the large well-to-aquifer hydraulic conductivity (K) difference of the engineered reactive media relative to the aquifer hydraulic conductivity (Wilson et al. 1997; Divine et al. 2013), a wide area of impacted groundwater passively flows into the screened well. Contaminants present in the flow sorb onto the reactive media where they are either immobilized or destroyed via biologi-

Article impact statement: Hydraulic performance of a novel horizontal well for passive in situ remediation validated in a field pilot study and numerical simulations.

doi: 10.1111/gwmr.12406

cal treatment from a solid organic material placed in the line of the flow. The treated groundwater then exits the well through the screen along the down-gradient sections of the well. The HRX Well approach can provide a rapid and dramatic reduction in contaminant mass flux, and it requires no above-ground treatment or footprint and limited ongoing maintenance. Divine et al. (2013) proposed simplified equations (design equations) described in the material and methods section for passive flow and capture in the HRX Well. To demonstrate the HRX Well concept, Divine et al. (2018a, 2018b) conducted a series of physical laboratory tests and numerical reactive transport modeling to evaluate its performance. Results from the laboratory tests confirmed the numerical model predictions as well as the well hydraulics (measuring flow and velocity) and contaminant treatment with granular activated carbon (GAC) and zerovalent iron (ZVI) (tracer test).

Limited literature to date exists (Hosseini et al. 2018) demonstrating the performance/remediation of impacted groundwater with a passive horizontal well filled with reactive media oriented in the direction of groundwater flow and will be the focus of this paper. Studies using passive wells have indicated that various parameters such as the type of reactive media within the well and its hydraulic conductivity, well geometry (diameter, well length), well spacing, and the number of wells influences their hydraulic performance and effectiveness in treating contaminants (Bortone et al. 2013; Hudak 2016, 2017). Hudak (2017) and Hosseini et al. (2018) also stressed the effect of the aquifer heterogeneity and complexity on groundwater flow path, contaminant distribution, containment, and removal.

HRX Well Reactive Transport Model (Simplified Equations)

This section describes the HRX Well reactive transport model by Divine et al. (2013). The HRX Well design model (simplified equations) is based on Darcy's Law. Darcy's Law governs the movement of fluid through a porous medium and is given as (Bear 1979)

$$Q = -KA\frac{\Delta h}{\Delta l} \tag{1}$$

where Q = volumetric flow rate (m^3/s or $feet^3$/s), A = cross-sectional area perpendicular to flow (m^2 or $feet^2$), K = hydraulic conductivity (m/s or feet./s), l = flow path length (m or feet), h = hydraulic head (m or feet), and Δ = denotes the change in h over the length, L.

For the HRX Well, the passive flow rate adapted from Darcy's Law is represented as

$$Q_{HRX} = K_{HRX}.\pi r_{HRX}^2.i_{HRX} \tag{2}$$

where K_{HRX} is the hydraulic conductivity of the media within the well, r_{HRX} is the radius of the well, and i_{HRX} is the hydraulic gradient of the well given as

$$i = \frac{\Delta h}{\Delta l} \tag{3}$$

where Δh = change in hydraulic head and Δl = distance between points where the head is measured.

In the HRX simplified model equation, the i_{HRX} can usually be assumed to be similar (but slightly lower) to the aquifer hydraulic gradient ($i_{Aquifer}$), because the well is horizontal and installed parallel to the groundwater flow (however i_{HRX} will generally be slightly less than $i_{Aquifer}$ in most cases). The average vertical capture zone width of the HRX Well is a function of the well diameter, aquifer thickness, and the ratio of the well and the aquifer hydraulic conductivity (Divine et al. 2018a), and is represented as shown (Divine et al. 2013)

$$W_{AVE} = \frac{Q_{HRX} = K_{HRX}\pi r^2 i_{HRX}}{K_{Aquifer} \times b_{Aquifer} \times i_{Aquifer}} = \frac{K_{HRX}\pi r^2}{K_{Aquifer} \times b_{Aquifer}} \tag{4}$$

where W_{AVE} = vertically averaged capture width; Q_{HRX} = flow through the HRX Well; $K_{Aquifer}$ = hydraulic conductivity of aquifer sand; $b_{Aquifer}$ = aquifer thickness; and $i_{Aquifer}$ = hydraulic gradient. Note for this derivation, the hydraulic gradient of the aquifer and HRX Well have been assumed to be approximately equivalent (which is valid for long wells with long screens); therefore, they cancel out. The average groundwater seepage velocity and average residence time are calculated by

$$v_{AVE} = \frac{K_{HRX} i_{HRX}}{n} \tag{5}$$

$$T_{AVE} = \frac{L_{HRX}}{v_{AVE}} \tag{6}$$

where n is the effective porosity of the well media and L_{HRX} is the median particle travel length of the particle through the media within the HRX Well.

The main objectives of this research include:

1. Test the HRX Well concept at a field PSS.
2. Compare simulations for two model types (discussed below) to field results.
   i. Simplified equations.
   ii. FEM model.
3. Determine if simplified model predictions are adequate for use in a field-scale conceptual design tool.

Materials and Methods

Approach

A PSS was conducted to test the HRX Well in a realistic physical setting by applying the reactive transport model (Divine et al. 2013, 2018a) to a field study. The FEM model was developed using data from the PSS to simulate groundwater flow in a hypothetical shallow unconfined aquifer. Details of the development of the FEM model software are provided in Supplementary Information 1 (Text S1). In all cases, a homogenous and isotropic aquifer with steady-state flow conditions is assumed. The parameters that were used in the PSS and FEM simulations are summarized in Table 1.

Results from the PSS were compared with the numerical simulation results and simplified equations to verify the

reactive transport model representing flow focusing and capture in the HRX Well.

PSS (Field Experiment)

The controlled field PSS was conducted at a field site at Clarkson University, Potsdam, New York, in a hydraulically isolated test pit. Figure 1 shows a representation of the HRX Well test pit design. The pit is representative of a relatively homogenous sand aquifer and was excavated to dimensions of 6.1 m (20 feet) long by 1.83 m (6 feet) wide by 1.83 m (6 feet) deep. Onwards the test pit will be described as the aquifer. The aquifer was hydraulically isolated from the surrounding media by an ethylene propylene diene monomer (EPDM) pond liner and was wet packed with sand in lifts of 1 m (Figure 2). Water was added to the aquifer after each lift to saturate the aquifer, which was then smoothed, scored, and allowed to settle before the next lift was added to prevent the occurrence of preferential flow paths.

Influent and effluent compartments comprised of gravel were emplaced at each end of the test pit to ensure uniform flow through the aquifer. The gravel compartments were separated from the sand using a geomembrane to avoid sand infiltration over time.

HRX Well Design

The HRX Well consists of 0.20 m (8-inch (")) diameter polyvinyl chloride (PVC) well screen casings that were purchased from Hole products and arrived at the site in different sections with a total length of 5.2 m (17 feet). The well had continuous slot screen openings of 0.508 mm (0.020"), and all screen to casing couplings were flush threaded. Teflon tape was wrapped around all connections, and both ends of the well were capped. While assembling the well, some sections were glued with PVC primer to prevent leaking. The horizontal well was installed during a 1-week period in August 2017 at an approximate depth of 1 m (3 feet) below ground level. The horizontal sections are approximately 2.44 m (8 feet) long, while the riser and the slanted sections together are approximately 2.74 m (9 feet) long and included a 0.61 m (2 feet) unscreened section (middle section). Details of the well sections and length are provided in Table S1. The well was wet packed with washed Filtrasorb-816 GAC, purchased from Calgon Corporation, in sections before assembly to form a single horizontal well. The sections were wet packed as follows. A slurry was made with GAC and water. The slurry was placed into the PVC pipe in lifts. For each lift, the emplaced slurry was agitated by hand to merge more homogenously with the underlying lift and reduce entrained air bubbles/pockets. Lastly, each lift was firmly tamped to ensure uniform packing. After the horizontal sections of the well were packed, an excavator was used to emplace the packed horizontal section of the well in the aquifer, ensuring that the well materials were in place (Figure 3a). The elbow and the slanted sections were then attached to the well, and packing continued until the well was completely packed and capped with a 0.20 m (8") flat ASTM S40 2TPI cap and plug (Figure 3b).

Table 1
Summary of Input Parameter for the FEM Model and PSS

Parameters	HRX Well	Aquifer
Flow rate (m^3/d)	1.13	1.77
Hydraulic conductivity (K, cm/s)	0.54	0.006
Porosity (n) (assumed)	0.55	0.35
Cross-sectional area (m^2)	0.03	3.34
Aquifer thickness (b, m)	—	1.83
Hydraulic gradient (i)	0.075	0.075

Monitoring Piezometers

An array of 40 25.4 mm (1") diameter piezometers was installed at different depths across and along the aquifer to monitor the pressure or water head in the aquifer (Figure 4). Details of the configuration, elevation, and distribution of the monitoring piezometers are presented in Figure S2. Water levels in the piezometers were measured using a Campbell Scientific CS 451 stainless-steel case submersible pressure transducer wired to a Campbell Scientific CR 1000

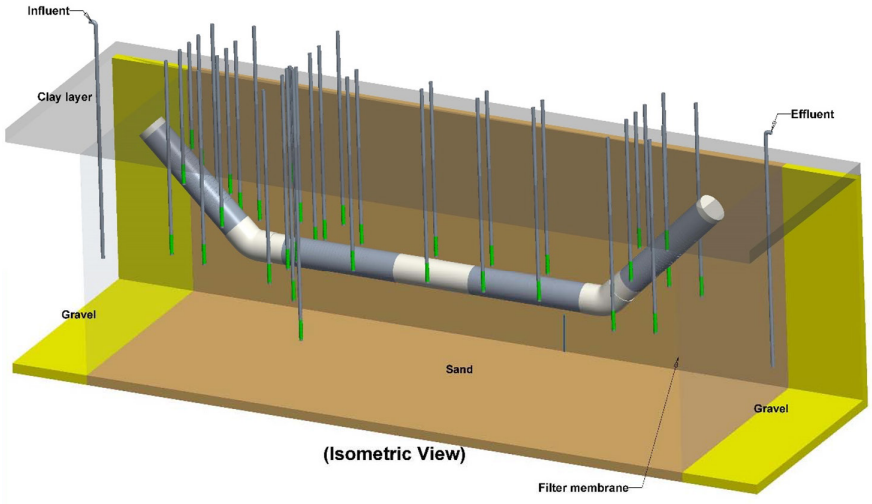

Figure 1. Representation of HRX Well® test pit design.

Figure 2. (a) Pilot-scale system test pit; (a) excavated pit was 6 feet deep by 6 feet wide by 20 feet long, lined with an EPDM pond liner, and (b) pit with packed sand before HRX well installation with 2-feet long gravel compartments at each end.

Figure 3. (a) Photograph of the packed horizontal well section with elbows emplaced in the aquifer and (b) photograph of fully packed well installed within the test pit.

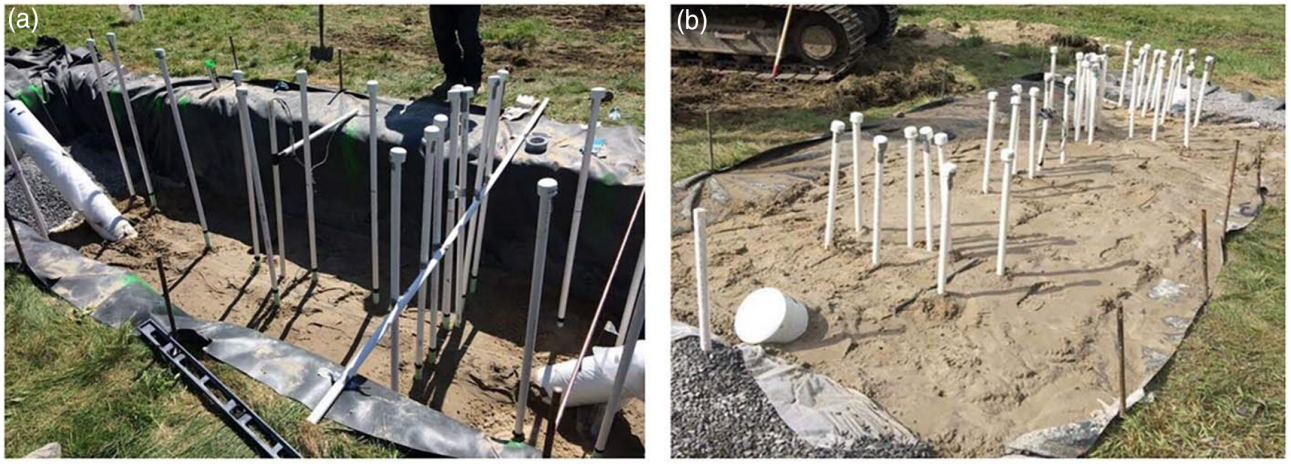

Figure 4. Photographs of piezometer placement during (a) and following (b) test pit construction.

data logger. The hydraulic heads measured in the piezometers are provided in Tables S2-S4.

Aquifer Operation

After installing the HRX Well and piezometers and packing the remaining sand surrounding the well in the aquifer, it was covered with a layer of gravel across the top. Water was introduced into the aquifer until it reached the surface to assure complete saturation. Once saturated, flow through the aquifer and well was established by pumping water from the gravel effluent end of the pit into a storage tank connected by a hose within a standpipe embedded in the gravel. Once a drop in the hydraulic head of approximately 0.46 m (1.5 feet) was measured in the effluent end of the aquifer, water was pumped from the storage tank into the influent gravel compartment at the same flow rate used to pump water out. Pumping continued, recirculating water through the pit until water levels in all piezometers reached steady state after approximately 2 days of continuous pumping. The measured pumping rate that maintained a consistent gradient of 0.075 across the pit was 2.9 m^3/d.

Effect of Hydraulic Gradient

A range of hydraulic gradients of 0.017, 0.033, 0.042, and 0.050 was induced across the aquifer by varying the hydraulic head at the effluent end to assess the influence of hydraulic gradient on the HRX Well hydraulic performance. Because the hydraulic gradient is the driving force for flow within an aquifer (Equation 3), resultant data are expected to show variations in water levels, flow rate, groundwater velocity (seepage velocity), and flow direction. The seepage velocity v (cm/s) was calculated using the one-dimensional form of Darcy's Law and assumed a homogenous condition.

Hydraulic Conductivity

The falling head method was used to calculate the hydraulic conductivity of the aquifer sand and reactive media in the well (e.g., Fetter, 2001). The K across the cores in the HRX Well was assumed to be the same because the well was filled with the same type of reactive media (GAC).

Data Analysis

The data obtained from the water level measurements were described using surfer software and presented on contour and surface plots. Data obtained from the PSS were used to evaluate the HRX well concept, including the well hydraulics and capture area (width).

FEM of the HRX Well

Problem Description

The groundwater flow equation without a source term in three-dimensional (3D) space:

$$\frac{S_s \partial h}{\partial t} = -\nabla \bullet q \tag{7}$$

for all $(x, y, z) \in \Omega$ where Ω is the whole aquifer, inclusive of the well, h is the hydraulic head to be evaluated, S_s is the specific storage, and q is the flux vector defined as $q = (q_x, q_y, q_z)^T$ where T is vector transpose, q_x, q_y, q_z are flux along x, y, and z coordinate axes, ∇ is the gradient operator defined as $\nabla = \left(\frac{\partial}{\partial x}, \frac{\partial}{\partial y}, \frac{\partial}{\partial z}\right)^T$. Using Darcy's Law, Equation 7 can be rewritten as

$$\frac{S_s \partial h}{\partial t} = -\nabla \cdot \left(-K \nabla h\right) \tag{8}$$

where K is the hydraulic conductivity matrix defined as $K = diag(K_x, K_y, K_z)$, where K_x, K_y, K_z are the values of hydraulic conductivity along x, y, and z coordinate axes. In this paper, the steady-state form of the groundwater flow treated by the HRX Well in a test pit is simulated, and the governing equation becomes

$$\nabla \cdot \left(K \nabla h\right) = 0 \tag{9}$$

Figure 5 is used to illustrate boundary conditions and show the segments of the HRX Well. The HRX Well is along the x-direction and is installed in the middle of the x-and y cross-section view.

The left and right faces are both Dirichlet boundary conditions as

$$h(x) = h_l, x \in \partial\Omega_1 \tag{10}$$

$$h(x) = h_r, x \in \partial\Omega_2 \tag{11}$$

where h_l is hydraulic head on $\partial\Omega_1$, h_r is hydraulic head on $\partial\Omega_2$. $h_l > h_r$, so, the groundwater flows from left to right along the positive direction of the x axis. The other four faces of the test pit are all zero flux Neumann's boundary conditions

$$\frac{\partial h(x)}{\partial n} = 0, x \in \partial\Omega_3. \tag{12}$$

The entire well is a curved cylinder with a uniform diameter. Each segment of the well is denoted by a distinct color. The inlet and outlet screened sections are in blue, and the green part is unscreened (Figure 5). Groundwater is captured by the inlet screened section of the well because the permeability of the well media is higher than the aquifer permeability. Groundwater flows into the well through the well screens and the upgradient portion of the well and is

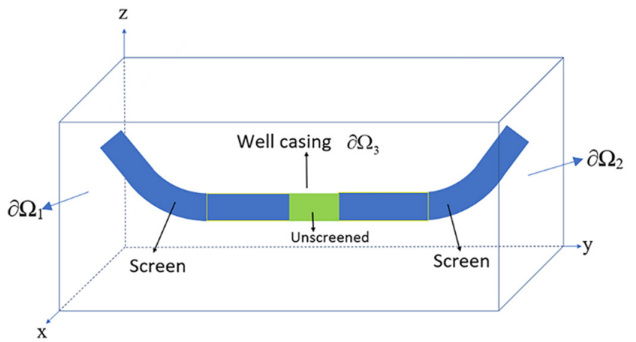

Figure 5. Boundary conditions of the test pit.

treated in situ as it flows through the HRX Well and exits the well through the screen along the downgradient sections (Divine et al. 2013, 2018a). The sealed HRX Well casing follows no flux Neumann's boundary condition.

Numerical Formulation

The hydraulic capture by the HRX Well was simulated using the FEM model based on tetrahedron meshes. The computational domain is represented as a multiple hydraulic conductivity environment. The horizontal well is installed in the middle of the aquifer with an equivalent hydraulic conductivity. The aquifer is uniform, that is, homogenous, and isotropic ($K_x = K_y = K_z$) with a hydraulic conductivity smaller than the well conductivity. Using the FEM method, the corresponding hydraulic conductivity is assigned to each element according to its attribute. Tetrahedrons are generated automatically, and the well structure can be manipulated without manual intervention.

To solve the partial differential equation (PDE) model, the Galerkin weak form is first applied to the governing equation (Equation 9). Thus,

$$\int_{\Omega} \delta h^T \nabla \cdot \left(\boldsymbol{K} \nabla h \right) = 0, \tag{13}$$

where δh is the hydraulic head variation along the HRX Well. Performing Gauss divergence theorem to the governing equation (Equation 9) and applying the zero flux Neumann's boundary condition yields

$$\int_{\Omega} \left(\nabla \delta h \right)^T K \left(\nabla h \right) d\Omega = 0, \tag{14}$$

The whole domain Ω is divided into n_e elements $\Omega_i^e, i = 1, 2, \ldots n_e$. The hydraulic head h of each point can be approximated by

$$h \approx N^i h_i \tag{15}$$

where $N^i(x) = \left[N_1^i(x) N_2^i(x) N_3^i(x) N_4^i(x) \right]$ is the linear shape function vector for the i-th element that the point belongs to, and h_i is the hydraulic head vector of the four vertices of the element. By substituting (Equation 15) into (Equation 14), the steady-state groundwater flow equation becomes

$$Gh = 0 \tag{16}$$

in which

$$G = \sum_{i=1}^{n_e} \int_{\Omega_i^e} \left(\nabla N^i \right)^T K_i \left(\nabla N^i \right) d\Omega = \sum_{i=1}^{n_e} V_i \left(\nabla N^i \right)^T K_i \left(\nabla N^i \right) \tag{17}$$

where K_i is the hydraulic conductivity matrix of i-th element Ω_i^e and V_i is the volume of Ω_i^e. After applying Dirichlet boundary conditions, one can obtain the hydraulic heads on all the nodes by solving the system.

Results and Discussion

This section discusses the results obtained from the PSS, FEM data analysis, and its comparison to the simplified design equations. The parameter default values used in this study are presented in Table 1.

Hydraulic Head and Capture Width: PSS and FEM

The majority of the discussion made in this subsection is from the results obtained at average hydraulic gradient, 0.075.

The PSS data analysis is based on the water level measurements made in each of the piezometers located in different positions in the sand aquifer. The total hydraulic head was obtained by adding the elevation head, z, and pressure head from the pressure transducer. As water was being recirculated through the aquifer while maintaining an average gradient (0.075) across the aquifer, the gradient changed markedly at the HRX Well entrance. The hydraulic gradient induced in the aquifer was determined by measuring the distance between the shallowest and deepest water levels in the piezometers parallel to the flow direction (Equation 3). A 3D surface plot of hydraulic heads measured in the aquifer is shown in Figures 6 and 7.

Based on measured hydraulic head values and interpolation between measured points, the maximum capture width of the well was estimated at about 1.0 m (40″) from the contour plot shown on Figure 7. This capture width is approximately five times greater than the well's diameter of 0.2 m (8″). It should be noted that there are software-related limitations with the geostatistical method (surfer software) that was used to plot the potentiometric surface map. In the PSS, there were no piezometers within the HRX Well, so there may be limitations on the accuracy of the interpolation and interpretation made by the software displayed in Figures 6 and 7. For instance, looking at the head values in the 3D surface plot (Figure 6), it appears as if water would flow out of the well, however, this is not true and is a function of the geostatistical interpretations because there are no direct head measurements within the HRX Well. Also, in Figure 7, the head contours do not intersect orthogonally as

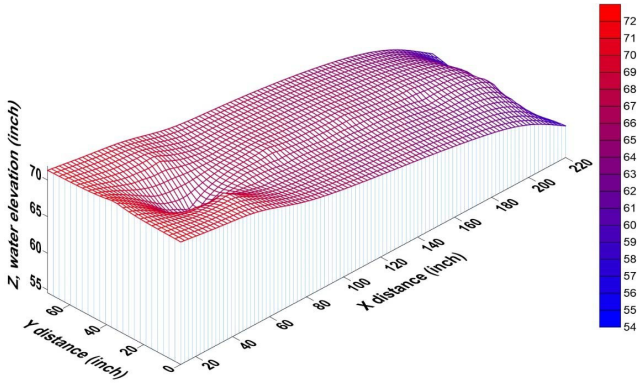

Figure 6. Three-dimensional surface plot of hydraulic head values measured at 40 points within the test pit. Water levels are in inches. The well capture zone is indicated by the dip in water levels toward the influent end of the aquifer, between 40 and 60 inches on the "distance" axis.

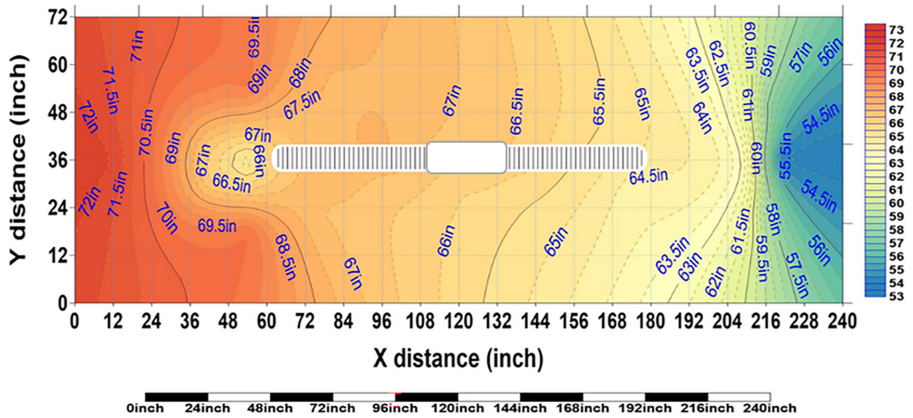

Figure 7. Contour plot of hydraulic head values measured at points within the aquifer. Water levels are in inches. The well capture zone is indicated by the steep gradient at the influent end of the HRX well, between 40 and 60 inches on the "*x* distance" axis.

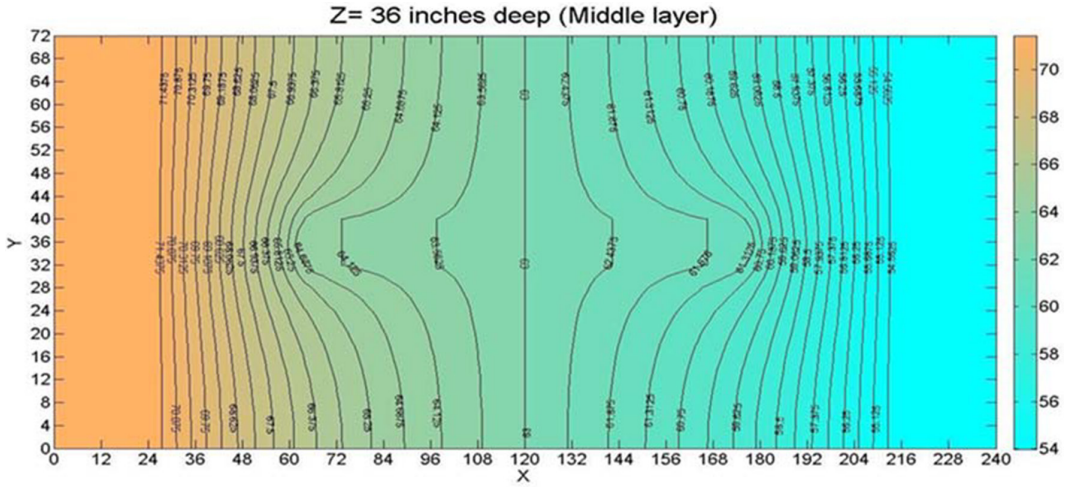

Figure 8. Contour plot of the FEM hydraulic heads at a hydraulic gradient of 0.075, *x* = *x* distance in inches along the test pit and *y* = *y* distance in inches across the test pit.

they should because the model was generated from a kriging-based geostatistical interpretation of water levels.

Through the FEM simulation, the contour plot of the hydraulic heads at a hydraulic gradient of 0.075 was obtained (Figure 8). Note that unlike that of the PSS, the contour heads are orthogonal because the FEM is a flow model, while surfer is a geostatistical model. Figure 9 shows the capture zone and streamlines of the groundwater flow. The groundwater flow is perpendicular to the contour lines. The capture zone is enclosed by red streamlines and was estimated by measuring the width of the streamlines flow into the well. The results of the numerical model showed that for an isotropic and homogenous aquifer, a capture width of 39 inches, 4.9 times greater than the HRX Well diameter, is obtained for a hydraulic gradient of 0.075 and hydraulic conductivity ratio of 90:1 (Kwell/Kaquifer).

Effect of Hydraulic Gradient: PSS and FEM

The relationship between the hydraulic gradients tested and the flow velocity for the PSS and FEM is shown in Figure 10. The numerical simulation results by FEM and PSS indicated that the flow velocity in the HRX Well increased with an increasing hydraulic gradient as would be expected. This is because the hydraulic gradient is the driving force of water movement and is proportional to the groundwater velocity; thus, groundwater flow is faster with a larger hydraulic gradient. It is worthy to note that the groundwater velocity is also dependent on hydraulic conductivity. Consequently, with the increase in velocity, the residence time of the impacted groundwater within the HRX Well is expected to shorten because the minimum average residence time is estimated from Equation 6. Therefore, balancing the achievable treatment residence time within the reactive media in the HRX Well with the anticipated hydraulic residence time is a critical design consideration for achieving remedial objectives.

In the PSS, comparing capture widths at different hydraulic gradients, the measured capture width obtained from surfer contour plots (Figure S3). indicates that the capture width does not change with a varying hydraulic gradient (i.e., the hydraulic gradient does not influence the capture width) The FEM simulation results shown in Figure 11 also suggest that the capture width is not sensitive to the change in the hydraulic gradient (Li 2019; Li et al. unpublished data 2020).

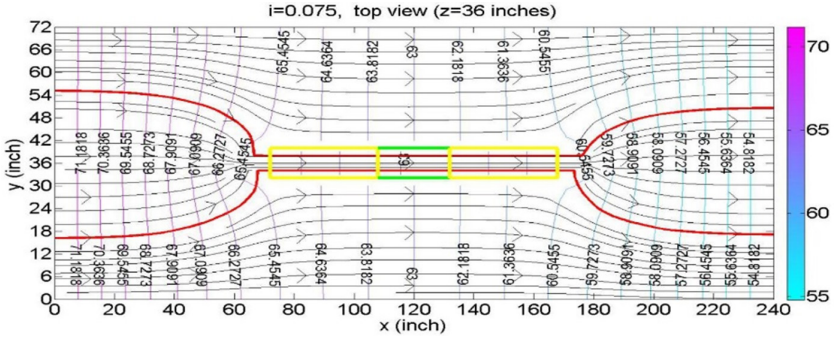

Figure 9. Capture zone of the HRX well (z = 36 inches) at average hydraulic gradient = 0.075.

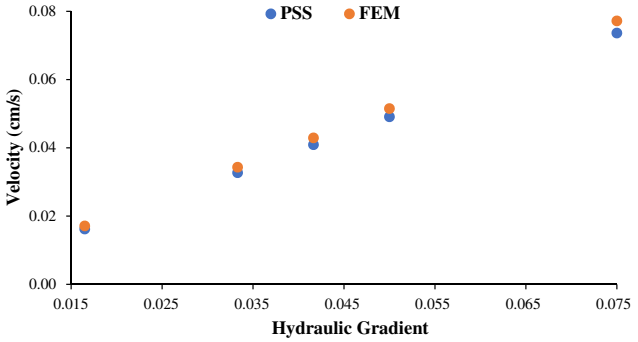

Figure 10. Comparison of calculated velocity (field) and FEM velocity in media at different hydraulic gradient i = 0.017, 0.033, 0.042, 0.05, 0.075.

These observations corroborate the expanded simplified equation for the vertical capture width (Equation 4), which assumes that the hydraulic gradient of the HRX Well is similar but slightly lower than that of the aquifer. Therefore, the ambient aquifer hydraulic gradient will not theoretically affect the capture width of the HRX Well (but it is positively correlated with the flow and velocity through the well).

Simplified Equations

Calculations were made using the simplified equations to explore the validity of the use of the design equations to represent flow and capture in the HRX Well. Darcy's Law was used to estimate the flow rate through the HRX Well in the aquifer. The GAC hydraulic conductivity was measured to be 0.54 cm/s, and the induced gradient in the aquifer was 0.075. Considering the well's 0.1 m (4-inch radius), the calculated flow in the well was 1.13 m^3/d ($Q_{HRX} = K_{HRX}\pi r^2 i$). Subtracting this from the pumping rate of 2.9 m^3/d ($Q_{Total} = Q_{HRX} + Q_{aquifer}$) using a mass balance approach provided the flow through the surrounding aquifer of 1.77 m^3/d ($Q_{aquifer} = Q_{Total} - Q_{HRX}$). The calculated average capture width (Equation 4) based on these values was 1.6 m (63″), which is greater than that interpolated from test pit data (1.0 m). The percentage of water captured by the well relative to the aquifer was compared using the flow rate from Darcy's Law using equation.

$$\frac{Q_{HRX}}{Q_{Total}} \times 100 \tag{18}$$

The well captured approximately 39% of the flow through the aquifer based on its dimensions and measured GAC conductivity. There is uncertainty, however, in the packed hydraulic conductivity of the GAC. For reference, the well volume is 0.5% of the total test pit.

Comparison of Results: PSS, FEM, and Simplified Equations

Results obtained from the field test were compared to the numerical model simulations to assess the adequacy of the conceptual model. The comparison was made at hydraulic gradient = 0.075. Figure 12 shows a comparison of hydraulic heads at well depth = 1 m (36″ in) for the PSS and numerical model.

Note at z = 1 m (36 inch) and y = 1 m (36″) may not be exact for the field data because the FEM model assumes hydraulic head measured in the well while the field data is obtained from piezometers installed outside the well but at the same depth.

In Figure 12, differences in hydraulic heads are seen between each data set, especially for the field data; this is likely because, in models, uniform values are assigned to some parameters, for example, the hydraulic conductivity of the aquifer sand. However, in the field, there may be variations in these values (aquifer heterogeneity and complexity). For example, during the installation of the piezometers, there were disturbances to the aquifer, which may have caused compaction and may lead to preferential flow in the aquifer. Also, as mentioned, the model assumes in well measurements while field measurements were made outside of the well. It is observed in Figure 12 that as the distance increases along the x-direction, the nonlinearity of the hydraulic head profiles increases, especially for the field data.

The relative error between the numerical simulation and the field data was calculated for hydraulic heads at varied hydraulic gradients. The relative error of hydraulic heads is defined as

$$\varepsilon(\%) = \frac{h_0 - h}{h} \tag{19}$$

where h_0 is the field measured hydraulic heads, and h is the numerical hydraulic heads.

For the evaluation of hydraulic heads at different hydraulic gradients, the relative was calculated for the FEM model and the field results whose input parameters were the same.

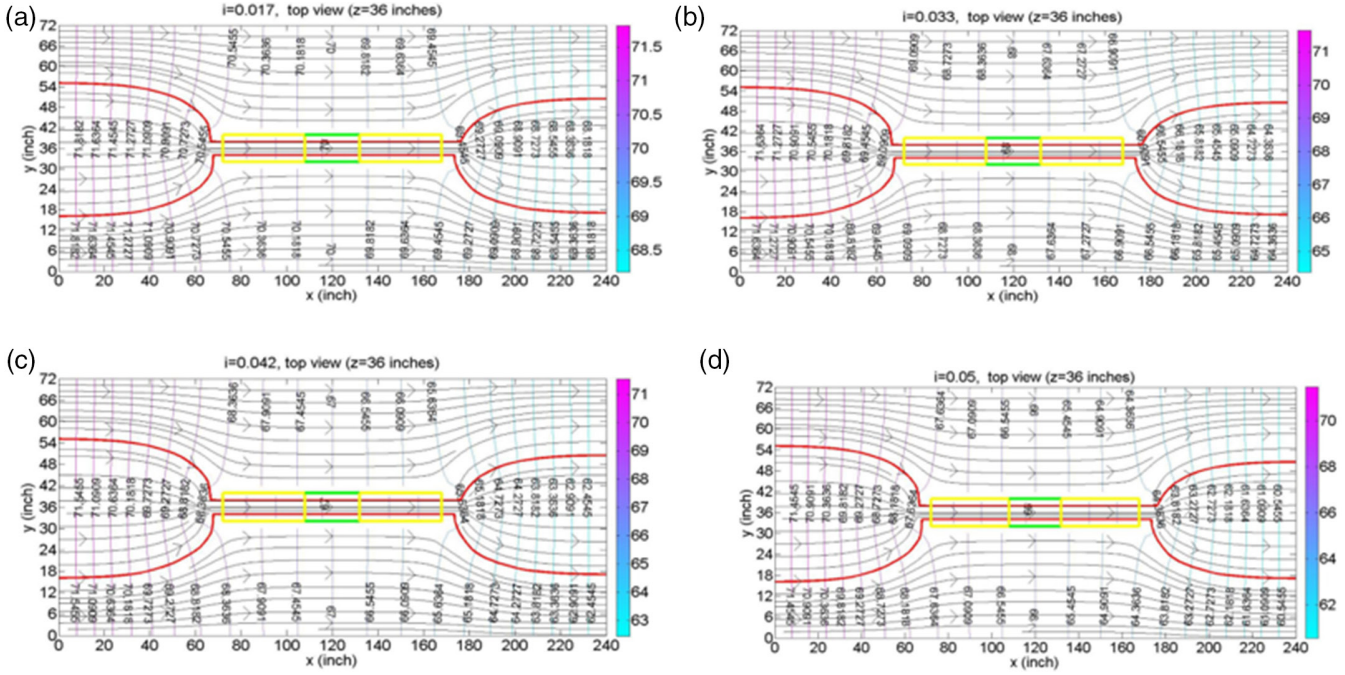

Figure 11. Capture zone of the HRX well (z = 36 inches) at average hydraulic gradient = 0.017, 0.033, 0.042, and 0.050.

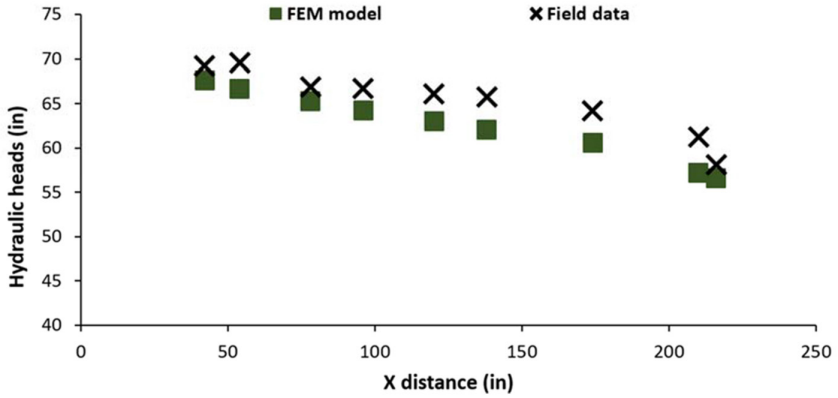

Figure 12. Comparison between field and modeled results at z = 36 inches and y = 36 inches.

The maximum relative error obtained was 4.3% and was observed to increase with gradient. Leão and Gentry (2011) have also reported an exponential increase in error with increasing hydraulic gradient. These errors may be a result of estimation errors, measurement errors (fluctuations in pumping rate), or local variations in aquifer properties (Devlin and McElwee 2007). The maximum relative error result is <5%, which indicates that the measured and simulated head values are in good agreement and is said to be acceptable for real-world applications (Ayvaz and Karahan 2008).

For the average capture width of the HRX Well, there was a good agreement between the FEM model (≈1.0 m) and the PSS (1.0 m) as compared to the simplified equations (1.6 m). The effect of inconsistent boundary condition assumptions may have influenced the differences observed in the results of these various scenarios (measured, calculated, modeled). For instance, the simplified equations assume an infinite domain size, while for the field and numerical simulations, the domain size is finite. The incorporation of domains beyond the depths where measurements and mapping are possible/available (like in the field), may have played a role in the differences between the field and numerical model results. Factors other than the boundary conditions, such as aquifer characterization and operating parameters, may have influenced the uniformity of results obtained from the field, simplified equations, and numerical simulations. Transient stress, such as infiltration, pumping, and change in weather cycles, which were not simulated in the models, may also contribute to the differences in obtained results. A summary of the performance metrics for the simplified equations (HRX Well design equations), numerical simulation, and field data is shown in Table 2. Both the observed (interpolated), modeled, and calculated values are significantly greater than the 0.2 m (8") diam-

Table 2
Performance Metrics for the Simplified Equations (HRX Well Design Equations) Numerical Simulations and Field Data

Parameters	Simplified Equations $i = 0.075$	FEM Model $i = 0.075$	Measured Value (Field) $i = 0.075$
Capture width (m)	1.6	≈1.0	1.0
Ratio of capture area	0.88	0.54	0.56
Velocity (cm/s) @ $i = 0.075$	0.09	0.07	N/A
Flow rate (m^3/d)	1.13	1.13	1.13 (calculated)

eter of the well, indicating significant passive capture by the well. These results demonstrate the validity of the simplified equations for the development of a field-scale design tool.

Overall, given the complex relationship between numerical models and natural systems, the agreement between the simplified equations, field measurements, and numerical simulation results are encouraging. There is a good agreement between the capture width obtained with the FEM model, the field results, and the simplified design equations. It is important to keep in mind that the use of the numerical simulations and simplified models are site-specific because some parameters such as hydraulic conductivity, grid dimensions, and boundary conditions incorporated into models are specified to represent a particular geographical area and may not provide accurate predictions or be applicable in another geographical area.

Conclusions

In the present work, the design equations and hydraulic performance of a novel technology "the HRX Well" were tested in different settings; field (PSS) and numerical simulations. Results from this study are in good agreement with the existing hydraulic theory (Divine et al. 2013), which predicts that the capture zone is a function of the reactive media and aquifer permeability. And that the HRX Well effectively captures and treats a significant amount of impacted groundwater.

Considering the effect of inconsistent boundary conditions, uncertainties, and parameter variations: the aquifer and well media porosity, in situ hydraulic conductivity, hydraulic heads in the well (as piezometer readings were taken only from the aquifer) and flow in the well, it would appear that an adequate agreement was achieved between the field, simplified equations, and numerical simulation results. These observations confirm the adequacy of the simplified equations for conceptual-level design while the comparative difference between the well diameter and the resultant capture widths demonstrates the effectiveness of the HRX Well for passive flow and capture of a substantial amount of water from a contaminated aquifer. Findings from this study could help provide guidance in the conceptual design of a field study for effective implementation and management of the HRX Well in the groundwater remediation field.

Currently, based on the validation of the HRX Well concept by the PSS and numerical simulations, the HRX Well has been implemented at a trichloroethylene (TCE) contaminated site in Vandenberg Air force Base, California using a 152 m-long (550 feet), 0.31 m (12-inch) diameter well containing zero-valent-iron media cartridges. Results to date show significant TCE concentration reductions (>95%) passing through the HRX Well with treatment width exceeding 15 m (50 feet).

The scope of this study was to fundamentally test the hydraulics of the HRX Well in a simplified setting, so we focused on an isotropic and homogenous condition. However, more complicated specific heterogeneity and isotropic conditions should be evaluated in the future or based on site-specific conditions to understand the role of these complexities.

Acknowledgments

The authors would also like to thank Nageshrao Kunte at Arcadis and Dr. J.F Devlin and Billy Hodge at Kansas University for their assistance during the well installation. Funding and support for this work have been provided through the U.S. Department of Defense Strategic Environmental Research and Development Program (SERDP) and Environmental Security Technology Certification Program (ESTCP) programs (projects ER-2423 and ER-201631).

Authors' Note

The author(s) does not have any conflicts of interest.

Supporting Information

Additional Supporting Information may be found in the online version of this article. Supporting Information is generally not peer reviewed.

Appendix S1 Supporting Information.

References

Allouche, E.N., S.T. Ariaratnam, and K.W. Biggar. 1998. Environmental remediation using horizontal directional drilling: Applications and Modeling. *Practice Periodical of Hazardous, Toxic, Waste Management* 2, no. 3: 93–99. https://doi.org/10.1061/(ASCE)1090-025X(1998)2:3(93)

Ariaratnam, S.T., and E.N. Allouche. 2000. Remediation of contaminated sites using horizontal directional drilling. In *Construction Congress VI*, 435–444. Reston, Virginia: American Society of Civil Engineers. https://doi.org/10.1061/40475(278)47

Ayvaz, M.T., and H. Karahan. 2008. A simulation/optimization model for the identification of unknown groundwater well locations and pumping rates. *Journal of Hydrology* 357, no. 1–2: 76–92.

Bear, J. 1979. Hydraulics of Groundwater. New York: McGraw-Hill.

Bortone, I., A. Di Nardo, M. Di Natale, A. Erto, D. Musmarra, and G.F. Santonastaso. 2013. Remediation of an aquifer polluted with dissolved tetrachloroethylene by an array of wells filled with activated carbon. *Journal of Hazardous Materials* 260, no. September: 914–920. https://doi.org/10.1016/j.jhazmat.2013.06.050

Chen, C., J. Wan, and H. Zhan. 2003. Theoretical and experimental studies of coupled seepage-pipe flow to a horizontal well. *Journal of Hydrology* 281, no. 1–2: 159–171. https://doi.org/10.1016/S0022-1694(03)00207-5

Cleveland, T.G. 1994. Recovery performance for vertical and horizontal wells using semianalytical simulation. *Groundwater* 32, no. 1: 103–107. https://doi.org/10.1111/j.1745-6584.1994.tb00617.x

Divine, C.E., T. Roth, M. Crimi, A.C. DiMarco, M. Spurlin, J. Gillow, and G. Leone. 2018a. The horizontal reactive media treatment well (HRX well®) for passive in situ remediation. *Groundwater Monitoring & Remediation* 38, no. 1: 56–65.

Divine, C.E., J. Wright, J. Wang, J. McDonough, M. Kladias, M. Crimi, B.N. Nzeribe, J.F. Devlin, M. Lubrecht, D. Ombalski, B. Hodge, H. Voscott, and K. Gerber. 2018b. The horizontal reactive media treatment well (HRX well®) for passive in situ remediation: Design, implementation, and sustainability considerations. *Remediation Journal* 28: 5–16.

Divine, C.E., G. Leone, J. Gillow, T. Roth, H. Brenton, and M. Spurlin. 2013. Horizontal in-well treatment system and source area bypass system and method for groundwater remediation. U.S. Patent US8596351 B2. Alexandria, Virginia: Patents and Trademarks Office.

Devlin, J.F., and C.D. McElwee. 2007. Effects of measurement error on horizontal hydraulic gradient estimates. *Groundwater* 45, no. 1: 62–73. https://doi.org/10.1111/j.1745-6584.2006.00249.x.

Fetter, C.W. (2001) Upper Saddle River, 4th edn. NJ: Prentice Hall,

Furukawa, Y., K. Mukai, K. Ohmura, and T. Kobayashi. 2017. Improved slant drilling well for in situ remediation of groundwater and soil at contaminated sites. *Environmental Science and Pollution Research* 24, no. 7: 6504–6511. https://doi.org/10.1007/s11356-016-8283-8

Hantush, M.S., and I.S. Papadopulos. 1962. Flow of ground water to collector wells. *Journal of the Hydraulics Division, Proceedings of the American Society of Civil Engineers* 88, no. HY5: 221–244. https://cedb.asce.org/CEDBsearch/record.jsp?dockey=0012595

Hosseini, S.M., T. Tosco, B. Ataie-Ashtiani, and C.T. Simmons. 2018. Non-pumping reactive wells filled with mixing nano and micro zero-valent iron for nitrate removal from groundwater: Vertical, horizontal, and slanted wells. *Journal of Contaminant Hydrology* 210, no. March: 50–64. https://doi.org/10.1016/j.jconhyd.2018.02.006

Hudak, P.F. 2017. Large-diameter, non-pumped wells filled with reactive media for groundwater remediation. *Environmental Earth Sciences* 76, no. 19: 667. https://doi.org/10.1007/s12665-017-7029-3

Hudak, P.F. 2016. Evaluation of non-pumped wells with slurry cutoff walls for containing and removing contaminated groundwater. *Environmental Earth Sciences* 75, no. 1: 67. https://doi.org/10.1007/s12665-015-4932-3

Koenigsberg, S.S., E.R. Piatt, and L.I. Robinson. 2018. New perspectives in the use of horizontal wells for assessment and remediation. *Remediation* 28, no. 4: 45–50. https://doi.org/10.1002/rem.21575

Kompani-Zare, M., H. Zhan, and N. Samani. 2005. Analytical study of capture zone of a horizontal well in a confined aquifer. *Journal of Hydrology* 307, no. 1–4: 48–59. https://doi.org/10.1016/J.JHYDROL.2004.09.021

Laton, W.R. 2019. New perspectives on horizontal to vertical well ratios for site Cleanup. *Remediation Journal* 30, no. 1: 27–31. https://doi.org/10.1002/rem.21628

Leão, T.P., and R. Gentry. 2011. Numerical modeling of the effect of variation of boundary conditions on vadose zone hydraulic properties. *Revista Brasileira de Ciência do Solo* 35, no. 1: 263–272. https://doi.org/10.1590/s0100-06832011000100025

Li, Wen. 2019. Meshfree methods based on radial basis functions for solving partial differential equations: from strong form to weakened weak form. Potsdam, New York: PhD dissertation, Clarkson University.

Lubrecht, M.D. 2012. Horizontal directional drilling: A green and sustainable technology for site remediation. *Environmental Science & Technology* 46, no. 5: 2484–2489. https://doi.org/10.1021/es203765q

Payne, Fred C., Joseph A. Quinnan, and Scott T. Potter. 2008. Remediation hydraulics. *Remediation hydraulics*. Boca Raton, Florida: CRC Press. https://doi.org/10.1201/9781420006841.

Sawyer, C.S., and K.K. Lieuallen-Dulam. 1998. Productivity comparison of horizontal and vertical ground water remediation well scenarios. *Groundwater* 36, no. 1: 98–103. https://doi.org/10.1111/j.1745-6584.1998.tb01069.x

Wilson, R.D., D.M. Mackay, and J.A. Cherry. 1997. Arrays of unpumped wells for plume migration control by semi-passive in situ remediation. *Groundwater Monitoring & Remediation* 17, no. 3: 185–193. https://doi.org/10.1111/j.1745-6592.1997.tb00594.x

Zhan, H., and V.A. Zlotnik. 2002. Groundwater flow to a horizontal or slanted well in an unconfined aquifer. *Water Resources Research* 38, no. 7: 13–1–13–11. https://doi.org/10.1029/2001WR000401

Zhan, H. 1999. Analytical study of capture time to a horizontal well. *Journal of Hydrology* 217, no. 1–2: 46–54. https://doi.org/10.1016/S0022-1694(99)00013-X

Biographical Sketches

***Blossom N. Nzeribe**, corresponding author, PhD, MS (Civil and Environmental Engineering) Clarkson University, MS (Environmental Management) Coventry University, BS (Biochemistry) University of Port Harcourt. She is Environmental Engineer, GSI Environmental Inc., 9600 Great Hills Trail, Austin, TX 78759; bnzeribe@gsi-net.com*

***Wen Li**, PhD (Applied Mathematics), Clarkson University, MS (Applied Mathematics), Taiyuan University of Technology, BS (Information and Computer Science), Taiyuan University of Technology. She is Assistant Adjunct Professor, Department of Mathematics, University of California, Los Angeles, CA 90095; wenli@math.ucla.edu*

***Michelle Crimi**, PhD (Environmental Science and Engineering), Colorado School of Mines, MS (Environmental Health), Colorado State University, BS (Industrial Hygiene and Environmental Toxicology), Clarkson University. She is Director and Professor of Engineering & Management, Clarkson University, 8 Clarkson Ave, Potsdam, NY 13699; mcrimi@clarkson.edu*

***Guangming Yao**, PhD (Computational Science [mathematics]), University of Southern Mississippi, MS (Mathematics [Nonlinear Analysis]), Harbin Normal University, BS (Mathematics and Applied Mathematics), Harbin Normal University. She is Associate Professor/ Executive Officer, Department of Mathematics, Clarkson University, 8 Clarkson Ave, Potsdam, NY 13699; gyao@clarkson.edu*

Craig E. Divine, *PhD (Geochemistry) Colorado School of Mines, MS (Watershed Science) Colorado State University, BS (Biology) Wheaton College, Vice President, Arcadis, Irvine, CA. He can be reached at Arcadis, 320 Commerce, Suite 200, Irvine, CA 92602; craig.divine@arcadis.com*

Jeffrey McDonough, *PE (Environmental Engineering) New Jersey, MS (Environmental Engineering) Pennsylvania State University, BS (Civil and Environmental Engineering) Pennsylvania State University, Technical Expert and Associate Vice President, Arcadis, Highlands Ranch, CO. He can be reached at 630 Plaza Drive Suite 200 Highlands Ranch, CO 80129; jeffrey.mcdonough@arcadis.com*

Jack Wang, *MS (Hydrogeology) University of Nebraska Lincoln, BE (Hydrology and Water Resources Engineering), Chang' An University. He is with Arcadis, 7550 Teague Rd., Hanover MD 21076. USA; jack.wang@arcadis.com*